REFERENCES
Berliner, L. J., Grunwald, J., Hankovsky, H. O., & Hideg, K. (1982) *Anal. Biochem. 119*, 450-455.
Bradley, E. K., Thomason, J. F., Cohen, F. E., Kosen, P. A., & Kuntz, I. D. (1990) *J. Mol. Biol. 215*, 607-622.
Chakrabartty, A., Schellman, J. A., & Baldwin, R. L. (1991) *Nature 351*, 586-588.
Doi, M., & Edwards, S. F. (1986) *The Theory of Polymer Dynamics*, Clarendon, Oxford.
Gruenwald, B., Nicola, C. U., & Schwarz, G. (1979) *Biophys. Chem. 9*, 137-147.
Liff, M. I., Lyu, P. C., & Kallenbach, N. R. (1991) *J. Am. Chem. Soc. 113*, 1014-1019.
Marqusee, S., & Baldwin, R. L. (1987) *Proc. Natl. Acad. Sci. U.S.A. 84*, 8898-8902.
Marqusee, S., Robbins, V. H., & Baldwin, R. L. (1989) *Proc. Natl. Acad. Sci. U.S.A. 86*, 5286-5290.
Merutka, G., Lipton, W., Shalongo, W., Park, S. H., & Stellwagen, E. (1990) *Biochemistry 29*, 7511-7515.
Padmanabhan, S., Marqusee, S., Ridgeway, T., Laue, T. M., & Baldwin, R. L. (1990) *Nature 344*, 268-270.
Perico, A. (1989) *Biopolymers 28*, 1527-1540.
Soman, K. V., Karimi, A., & Case, D. A. (1991) *Biophys. J. 59*, 397a.
Tanford, C. (1968) *Adv. Protein Chem. 23*, 121-282.
Tirado-Rives, J., & Jorgensen, W. L. (1991) *Biochemistry 30*, 3864-3871.
Todd, A. P., & Millhauser, G. L. (1991) *Biochemistry 30*, 5515-5523.

Structural Basis for the Inactivation of the P54 Mutant of β-Lactamase from *Staphylococcus aureus* PC1†

Osnat Herzberg,*,‡ Geeta Kapadia,‡ Bernardo Blanco,§ Tom S. Smith,§ and Andrew Coulson§

Center for Advanced Research in Biotechnology, Maryland Biotechnology Institute, University of Maryland, 9600 Gudelsky Drive, Rockville, Maryland 20850, and Institute for Cell and Molecular Biology, University of Edinburgh, King's Building, Mayfield Road, Edinburgh EH9 3JR, U.K.

Received May 17, 1991; Revised Manuscript Received July 11, 1991

ABSTRACT: The crystal structure of a mutant protein of a class A β-lactamase from *Staphylococcus aureus* PC1, in which Asp179 is replaced by an asparagine (P54), has been determined and refined at 2.3-Å resolution (1 Å = 0.1 nm). The resulting crystallographic R factor ($R = \sum_h||F_o| - |F_c||/\sum_h|F_o|$, where $|F_o|$ and $|F_c|$ are the observed and calculated structure factor amplitudes) is 0.181 for 12 289 reflections with $I \geq \sigma(I)$ within the 6.0-2.3-Å resolution range. The mutated residue is located at the C-terminus of an extensive loop (the Ω-loop), remote from the active site, and results in a drastically reduced activity. Examination of the native and P54 structures reveals that the overall fold is similar, except that there is substantial disorder of the Ω-loop of P54. This is a consequence of the elimination of a salt bridge between Asp179 and Arg164 that links the two ends of the Ω-loop in native β-lactamase. It is associated with a difference in side-chain conformation between Asn179 in P54 and Asp179 in the native structure. An alternate interaction occurs in P54 between Asn179 and Ala69, adjacent to the catalytic Ser70. This disorder affects catalysis since some of the disordered residues, in particular Glu166, form part of the active site. Stopped-flow kinetic measurements of native and P54 β-lactamase with nirocefin confirm the prediction that disordering of the catalytic Glu166 in P54 makes deacetylation the rate-limiting step in hydrolysis: whereas the ratio of the acylation rate to the deacylation rate is about 1 in native β-lactamase, in P54 this value is ~600, mainly due to the reduction in the deacetylation rate. The acylation rate is reduced about 10-fold. Thus, the kinetics of P54 support the proposal that the acylation and deacylation steps in β-lactamase are functionally separate and are assisted by different amino acid residues.

The structure of a class A β-lactamase (EC 3.5.2.6) from *Staphylococcus aureus* PC1 has been determined (Herzberg & Moult, 1987) and refined at 2.0-Å resolution (Herzberg, 1991), providing atomic details of the overall fold and the active-site architecture of the enzyme. The spatial disposition of key active-site residues suggests a catalytic pathway that shares some features with the serine protease family (Kraut, 1975). The overall fold of the molecule highlights an extensive loop segment [the Ω-loop involving residues 164-178 according to the numbering scheme of Ambler (1979) and Ambler et al., (1991)], part of which is involved in the formation of the active site. In particular, we have proposed that Glu166, located on the loop, plays a catalytic role in the deacylation of the enzyme. The packing of the Ω-loop against the rest of the structure is rather loose, with nine internal solvent molecules in between (the "cave"). In addition, a very unusual sterically strained cis peptide has been identified between the catalytic Glu166 and Ile167 located on the Ω-loop. These two features suggest that the loop may be marginally stable and readily undergoes conformational transition. Our structural observations can be linked to Pain's folding experiments (Robson & Pain, 1976a,b; Adams et. al., 1980; Mitchinson

† Supported by NIH Grant R01-AI27175 and by a NATO travel grant.
* To whom correspondence should be addressed.
‡ University of Maryland.
§ University of Edinburgh.

0006-2960/91/0430-9503$02.50/0

Table I: P54 β-Lactamase Data Processing Statistics

shell lower limit (Å)	no. of reflections: possible	no. of reflections: missing	no. of observations	$\langle I/\sigma(I)\rangle$	fraction with $I \geq 2\sigma(I)$	R_{sym}[a]
4.18	2884	142	11760	51.9	0.97	0.046
3.32	2780	172	9931	28.1	0.93	0.072
2.90	2729	179	8986	13.0	0.84	0.122
2.63	2728	169	8209	7.0	0.73	0.175
2.44	2704	151	7456	4.6	0.62	0.219
2.30	2694	142	6138	3.0	0.50	0.267
total	16519	955	52480	18.4	0.77	0.084

[a] $R_{sym} = \sum_h \sum_l |\langle I\rangle - I(h)_l| / \sum_h \sum_l I(h)_l$ for symmetry-related observations.

& Pain, 1985; Creighton & Pain, 1980): The unfolding of the enzyme in urea or guanidinium chloride has been shown to be reversible and to exhibit partially folded enzymatically inactive states H and I. State H is stable at intermediate concentrations of the denaturant and retains much of the secondary structure of the native enzyme. It exists in rapid equilibrium with the unfolded state but in slow equilibrium with the native state, with a half-time of several minutes. The second intermediate, state I, has been identified on urea gradient polyacrylamide gel electrophoresis at low concentrations of urea. It appears to be in rapid equilibrium with state H and interconverts slowly with the native state. Its electrophoretic mobility suggests that state I is only slightly less compact than the native molecule. With the structure in mind, it is not unreasonable to suggest that one or both intermediates represent different conformational states of the Ω-loop.

The mutant P54 of β-lactamase PC1 was generated in vivo, isolated, and characterized by Novick (1963). Its activity is drastically reduced, yet it shows immunological cross-reactivity with the native enzyme. Sequence analysis by Ambler (1979) identified a point mutation replacing Asp179 by Asn in an otherwise apparently normal sequence. This is a conserved aspartate in all class A β-lactamase (Ambler, 1991) and is located on the C-terminus of the Ω-loop. The crystal structure of the native PC1 enzyme reveals that although some of the Ω-loop residues are involved in the formation of the active site, Asp179 itself is remote from it (the distance between the carboxylate group and the O^{γ} atom of the active-site serine is 12Å). Urea gradient polyacrylamide gel electrophoresis, circular dichroism, and sedimentation velocity experiments have led to the proposal that the mutant folds to a form that resembles state I such that it is slightly more expanded compared with the wild-type enzyme but contains a similar amount of secondary structure (Craig et al., 1985). These authors propose that P54, as well as a second mutant denoted P2, "represent a folding state of the native enzyme which is blocked at a point located after collapse of the already folded structural units into a globular shape, and close to the final reshuffling step that leads to the native state of the wild-type enzyme".

We have determined and refined the crystal structure of the P54 mutant at 2.3-Å resolution and have analyzed the structural changes associated with the inactivation of the enzyme. Kinetic experiments have been used to characterize the functional effect of the structural change.

Experimental Procedures

(A) *Crystallography*. The purification of the P54 mutant followed a protocol similar to that described for the native PC1 β-lactamase (Moult et al., 1985). Crystals were obtained by the hanging drop method from ammonium sulfate solutions, under the same conditions described previously (Herzberg & Moult, 1987). Like the original native enzyme crystals, they belong to space group *I*222 with cell dimensions that differ by 1–2%. For P54, a = 54.9 Å, b = 96.0 Å, and c = 137.8 Å; for native PC1, a =53.9 Å, b = 94.0 Å, and c = 139.1 Å.

X-ray data were collected on a Siemens area detector mounted on a three-circle goniostat. Kα Cu X-rays were generated with a Rigaku Rotaflex RU-200BH rotating anode. Data to 2.3-Å resolution were collected from one crystal. A unique set of structure factors was obtained by using the XENGEN data processing package (Howard et al., 1987). Details of the statistics of the data processing are summarized in Table I. The structure factors were scaled to absolute values with the computer program ORESTES, written by W. E. Thiessen and H. A. Levy.

The restrained-parameter least-squares refinement program of Hendrikson and Konnert (1980) was used to refine the P54 β-lactamase mutant structure, following a protocol similar to that used in the refinement of the native structure (Herzberg, 1991). The initial coordinates were those of the refined native molecule at 2.0-Å resolution (3BLM in the Brookhaven Protein Data Bank; Bernstein et al., 1977). Since the crystal cell dimensions differed by up to 2%, a six-dimensional rigid-body refinement was first carried out to properly position the molecule in the cell. Data between 10- and 5-Å resolution have been used. Next, 13 cycles of refinement have been carried out at 2.8-Å resolution, varying all atomic positions and individual temperature factors. A computer program version that includes a fast Fourier transform calculation was used (Finzel, 1987), refining data for which $I \geq \sigma(I)$. The resulting model was displayed together with three types of electron density maps: (a) a composite omit map (Bhat, 1988), (b) a map computed with the coefficients $|F_o| - |F_c|$ and calculated phases (F_o and F_c are the observed and calculated structure factor amplitudes), and (c) a map with coefficients $|F_o| - |F_c|$ and calculated phases. The E & S PS390 interactive graphics system was used, with the program FRODO (Jones, 1982). These initial maps showed that the side chain of the mutated residue Asn179 adopts a different conformation from that of Asp179 in the native structure. The model was modified accordingly. In addition, the initial electron density map associated with residues 163–175 was of poor quality. Therefore, these residues were omitted from the following cycles of refinement. Later, with the improvement of the maps, some of these amino acid residues were reinterpreted and added to the model. Data were added gradually increasing the resolution to 2.3 Å. Solvent molecules were added to the model after cycle 47 when the R factor was 0.221. These were assigned by a peak search of the difference Fourier map and were added to the coordinate set only if there were no substantial negative peaks in the vicinity, which would indicate possible errors in the model. The solvent molecules were refined as neutral oxygen atoms. None of them refined to unusually low temperature factors, which would indicate sites of ions heavier than water.

(B) *Kinetics*. The hydrolysis of β-lactam antibiotics catalyzed by class A β-lactamase has been shown to involve an

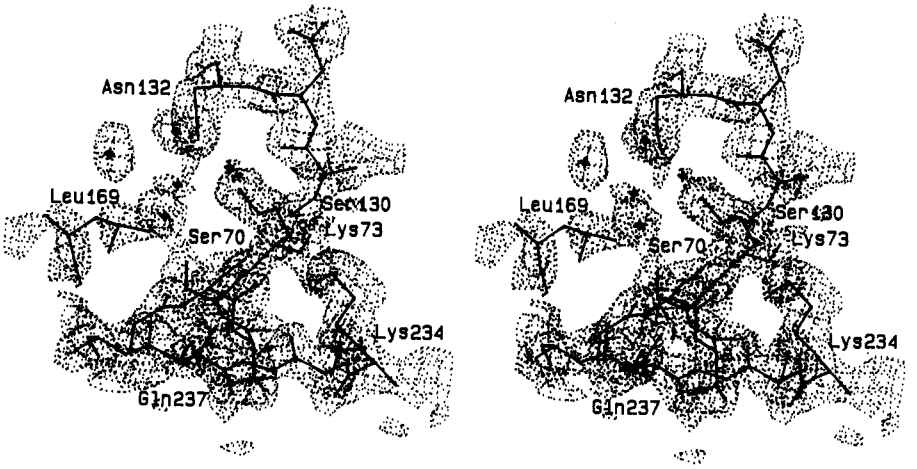

FIGURE 1: Stereoscopic view of the electron density map in the region of the active site. Calculated phases and the coefficients $2F_o - F_c$ are used. Contouring of the map is at 1σ level.

acyl-enzyme intermediate [for review, see Coulson (1985)], and recent kinetic studies [see, e.g., Christensen et al. (1990)] show that it may be described by the mechanism

$$E + S \underset{k_{-1}}{\overset{k_{+1}}{\rightleftharpoons}} ES \xrightarrow{k_{+2}} E\text{-acyl} \xrightarrow{k_{+3}} E + P \qquad (1)$$

The four rate constants of the reaction have been measured by Christensen et al. (1990) for various substrates and three classes A β-lactamases, including that from *Staphylococcus aureus* PC1. In all cases the three first-order rate constants, k_{-1}, k_{+2}, and k_{+3} are approximately equal. Under a range of conditions, the transient phases that can be observed in a stopped-flow machine for chromophoric substrates such as nitrocefin are dominated by k_{+2}. If k_{+2} is known (or if $k_{+2} \gg k_{+3}$), k_{+3} can be determined from steady-state experiments, since

$$1/k_{cat} = 1/k_{+2} + 1/k_{+3} \qquad (2)$$

Kinetic measurements under the steady-state conditions were made in a Perkin-Elmer PE320 UV/visible spectrophotometer, making absorbance changes at 500 nm (at nitrocefin) or 232 nm (for nonchromogenic substrates). Absorbance values (at 0.5 s or greater intervals) were collected by DEC MINC-11 system running under an RT11 operating system. Data were analyzed with FORTRAN programs running on the same system. Steady-state kinetic parameters were estimated from single progress curves by nonlinear least-squares fitting of the parameters K_m and K_m/V_{max} in the integrated Michaelis–Menten equations for a single-substrate reaction. Stopped-flow observations were made with an Applied Photophysics apparatus SF-17MV. All kinetics measurements were made in 0.1 M phosphate buffer, generally at pH 6.8, and at 25 °C. Protein concentrations were estimated from absorbance of solutions at 280 nm by using the value of ϵ_{280} 19 500 M^{-1} (Carrey & Pain, 1978).

The effect of pH on the k_{cat} of the hydrolysis of penicillin G by PC1 and P54 was measured by steady-state kinetics, recording the progress curve at 232 nm. Penicillin G was added to 0.1 M phosphate buffer, followed by the addition of the enzyme. Five pH conditions were explored: 5.0, 5.5, 6.0, 6.8, and 8.0. The effect of ammonium sulfate on the rate of catalysis was measured in a similar manner, with 0%, 30%, and 60% saturated ammonium sulfate solutions and 0.1 M phosphate buffer at pH 6.8.

RESULTS

(A) *Quality of the Structure.* Seventy-one least-squares cycles of refinement have been carried out. The final structure has an R factor ($R = \sum_h||F_o| - |F_c||/\sum_h|F_o|$, where $|F_o|$ and $|F_c|$ are the observed and calculated structure factor amplitudes) of 0.181 for the 12 289 reflections between 6.0- and 2.3-Å resolution for which $I \geq \sigma(I)$. The stereochemical parameters (Table II) are well within the range known from crystal structures of small peptides. The variation of the R factor with the resolution of the data is shown in Table III. Figure 1 shows a representative region of the electron density map with its associated model.

The refined model of the P54 mutant of β-lactamase includes most of the 257 amino acid residues of the protein molecule and 126 solvent molecules. However, there is no electron density associated with residues 165–168 (Tyr-Glu-Ile-Glu) and with the side chains of Arg164 and Asn170. Thus, these are omitted from the model. In fact, the crystallographic temperature factors in the region of the Ω-loop (residues 164–179) are substantially higher than those of the equivalent residues in the native structure (Figure 2). Neither in the PC1 nor in the P54 crystals are the Ω-loop residues

Table II: Deviation from Ideal Geometry at the End of the Refinement

	rms deviation from ideal values[a]
distance restraints (Å)	
bond distance	0.023 (0.025)
angle distance	0.042 (0.036)
planar 1–4 distance	0.040 (0.040)
plane restraint (Å)	0.024 (0.030)
chiral-center restraint (Å^3)	0.226 (0.200)
nonbonded contact restraints (Å)	
single torsion contact	0.238 (0.400)
multiple torsion contact	0.212 (0.400)
possible hydrogen bond	0.260 (0.400)
trans peptide torsion angle restraint ω (deg)	4.0 (5.0)

[a] The values in parentheses are the input estimated standard deviations that determine the relative weights of the corresponding restraints (Hendrickson & Konnert, 1980).

Table III: Crystallographic R Factor as a Function of Resolution

shell lower limit (Å)	R factor,[a] $I \geq \sigma(I)$	shell lower limit (Å)	R factor,[a] $I \geq \sigma(I)$
5.0	0.212	2.7	0.191
4.0	0.142	2.5	0.213
3.5	0.144	2.3	0.249
3.1	0.171	overall	0.181

[a] $R = \sum_h||F_o| - |F_c||/\sum_h|F_o|$.

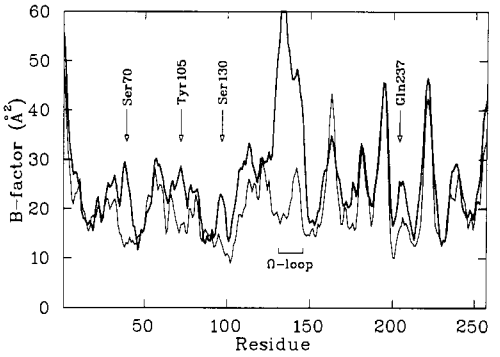

FIGURE 2: Variation in the average crystallographic temperature factors of main-chain atoms along the polypeptide chain of β-lactamase. Thick lines, the P54 mutant; thin lines, the native PC1 molecule. The numbering along the horizontal axis is sequential. Key residues in the active site are indicated by the Ambler (1979) numbering scheme.

involved in direct intermolecular contacts due to crystal packing. The functional significance of this disorder will be discussed below.

The electron density associated with the Ser130 side chain appears to be consistent with a larger side chain (Figure 1). Since Ser130 is conserved in all class A β-lactamases and interacts with the catalytic Ser70, we were especially concerned that this might indicate a second mutation, which would complicate the structural interpretation. However, the peptide T48 (Ambler, 1975) consisting of residues 121–137 according to Ambler numbering scheme (1991), has now been reisolated and analyzed from both PC1 and P54. The composition and the electrophoretic and chromatographic properties of the peptide were identical and in complete agreement with the overall sequence (R. P. Ambler, private communication).

The main-chain ϕ, ψ dihedral angle distribution is similar to that of the refined PC1 structure (Herzberg, 1991), with two β-carbon-containing amino acid residues in a sterically strained region [Ala69 at ϕ, ψ = (58°, −112°) and Leu220 at ϕ, ψ = (−100°, −127°)]. However, because of the disorder, the cis peptide between Glu166 and Ile167 located on the Ω-loop is not seen in the P54 crystal structure.

Less than half the number of solvent molecules have been assigned in the P54 crystal compared with that of the native. This may be associated with the somewhat lower resolution diffraction of the P54 crystal and its overall higher crystallographic temperature factor. Although independently determined, many of the solvent molecules of the native and of the P54 mutant crystal structures are similar. Seventy-two out of the 119 (60.5%) assigned solvent molecules in P54 are located within 1 Å of a solvent molecule identified in the native structure.

Table IV: Largest Differences in Main-Chain Atomic Positions between Native and P54 β-Lactamase[a]

residue	difference (Å)	location
Ala69	1.4	contacts the mutated Asn179 and is adjacent to the active-site Ser70
Ser70	1.0	catalytic residue
Ile97	1.0	in the vicinity of the disordered segment of the Ω-loop
Asn98	1.1	as Ile97
Asp100	1.2	as Ile97
Asp101	1.1	as Ile97
Ala104	1.1	as Ile97; also involved in the formation of the active-site gully
Pro162	1.7	by the N-terminus of the Ω-loop
Val163	2.3	as Pro162
Arg164	2.7	Ω-loop
Leu169	1.6	Ω-loop
Asn170	1.3	Ω-loop
Tyr171	1.6	Ω-loop
Gln237	1.6	active site; forms part of the oxyanion hole
Ala238	1.1	active site
Ile239	1.2	forms part of the active-site gully and contacts Tyr171 on the Ω-loop

[a] The superposition of native PC1 on P54 was carried out excluding the Ω-loop region. The resulting rotation matrix and translation vector were applied to the whole model. Residues with one or more main-chain atoms deviating by more than 1 Å are listed.

(B) *Structural Differences between Native and P54 β-Lactamase.* With the exception of the disordering of the Ω-loop, the overall fold of the P54 mutant is similar to that of the native β-lactamase molecule (Figure 3). When all but the Ω-loop atoms of P54 and of native β-lactamase are superpositioned, the root-mean-square (rms) deviation in atomic coordinates is 0.76 Å for all atoms. The rms deviation of the main-chain α-carbon atoms is 0.45 Å. The larger value obtained for the superpositioning of all atoms is primarily due to different conformations of surface side chains, in particular those of lysyl residues that are frequently associated with weak electron density and hence are difficult to interpret. Excluding amino acids that form the Ω-loop, there are only a few main-chain atoms whose positions deviate by more than 1 Å (Table IV). Such deviations are significant in a refined

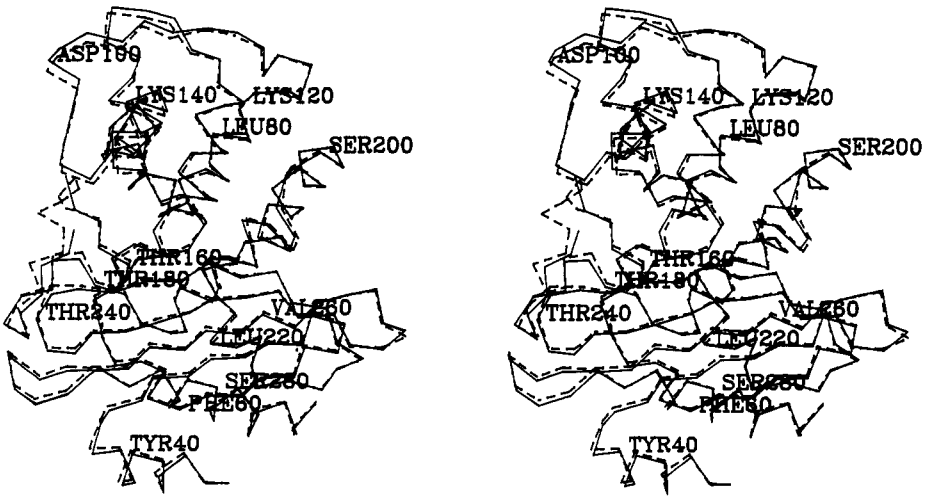

FIGURE 3: Stereoscopic representation of the superposition of native β-lactamase and the P54 mutant. Virtual bonds between α-carbon atoms of the native structure are shown in broken lines, and those of P54 are shown in continuous lines. The numbering is according to Ambler (1979).

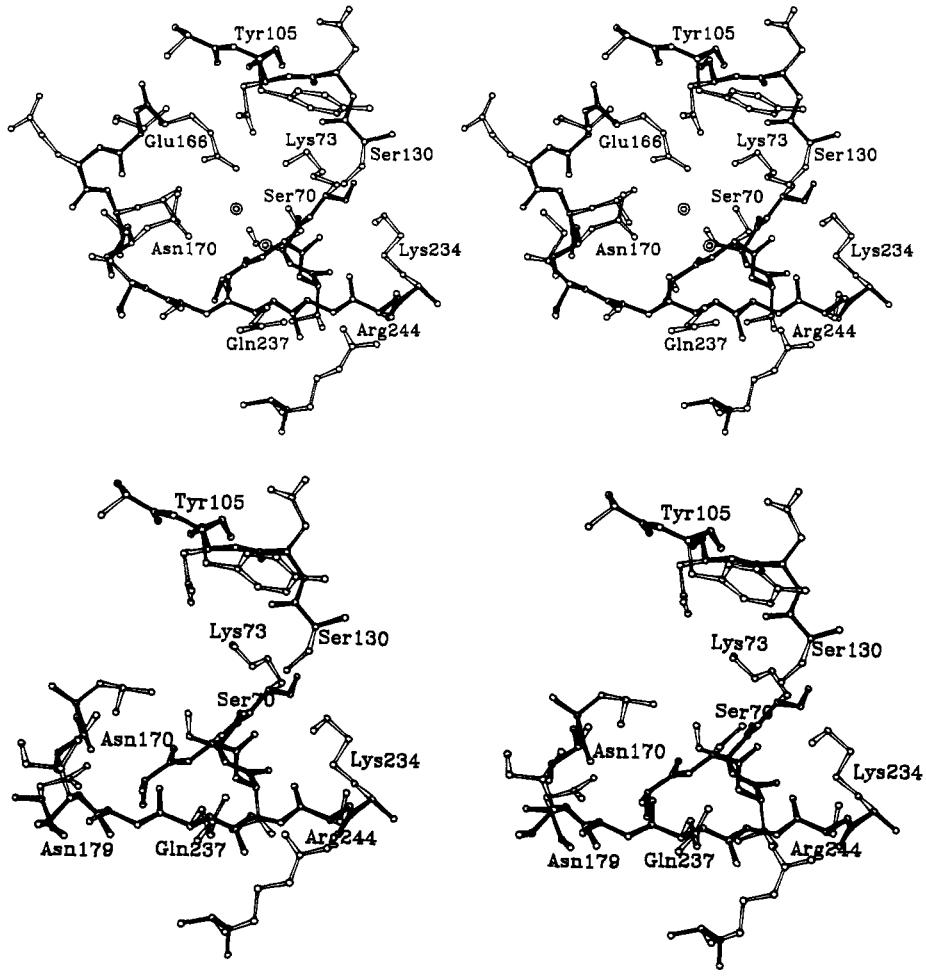

FIGURE 4: Stereoscopic representation of the active sites of PC1 and P54. Bonds between main-chain atoms are filled and those between side-chain atoms are open. (Top) PC1 β-lactamase. The two water molecules, one in the oxyanion hole and the other in a position suitable for the deacylation of the enzyme, are shown as double circles. (Bottom) P54 β-lactamase. Some amino acid residues on the Ω-loop are disordered and the above two water molecules are missing.

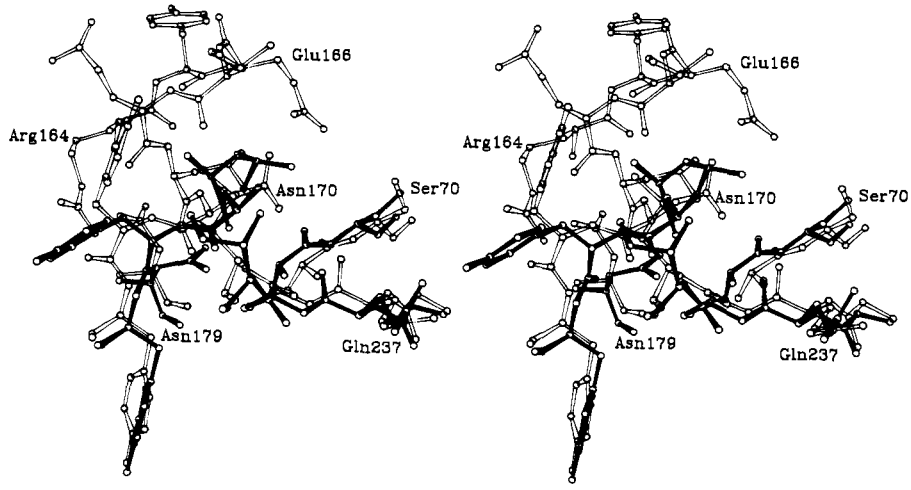

FIGURE 5: Comparison between PC1 and P54 β-lactamase in the vicinity of the active site, where the major differences are observed. Bonds of the PC1 molecule are open and those of the P54 are filled. The mutation is at position 179.

structure at 2.3-Å resolution. All are located in close proximity to the Ω-loop and are associated with the active-site depression.

The effect of the single mutation on the active-site residues is dramatic (Figures 4 and 5). Whereas in the native structure the side chain of Asp179 is oriented such that it forms a salt bridge with Arg131, in the P54 mutant the potential to form this salt bridge is eliminated due to the replacement of the aspartyl residue by the asparagine. Instead, Asn179 adopts an alternative side-chain conformation, such that is displaces one of a cluster of internal solvent molecules identified in the native structure between the Ω-loop and the rest of the molecule (Wat2 in the 3BLM coordinate set). This conformation facilitates a favorable electrostatic interaction between the side chain of Asn179 and the main-chain nitrogen atom of Ala69 (3.3 Å), shifting the nitrogen position toward Asn179. Consequently, the adjacent nitrogen atom of the catalytic Ser70

(Figure 5) that forms part of the oxyanion hole is shifted as well.

The residues closest in sequence to the disordered segment of the Ω-loop refined with high crystallographic temperature factors between 40 and 50 Å^2, indicating that they should not be considered reliable. They also deviate most from the native structure (Table IV). Nevertheless, the electron density of the Tyr171 side chain is consistent with it adopting a different conformation than seen in the native structure (Figure 5). This is associated with the different packing of this residue against the active-site edge β-strand residue, Ile239. The relative shift of Ala69, which packs underneath the oxyanion residue, Gln237, and the altered packing of Tyr171 against Ile239 result in the observed shift of Gln237. However, the positional shifts of the two nitrogen atoms that form the oxyanion hole are somehow coupled, such that given the accuracy of the structure determination it is impossible to conclude whether and to what extent the oxyanion hole is distorted.

The side chain of the active-site Ser70 refined with an altered conformation as compared to the native structure (Figure 5) and with a substantially higher crystallographic temperature factor: For example, the O^γ atom refined with $B = 3.4$ Å^2 in P54 and with $B = 20$ Å^2 in the native structure. Several other key residues in the active site also show increased apparent crystallographic temperature factors significantly above the overall higher temperature factor of the molecule, as can be seen in Figure 2. Associated with the higher mobility, two key solvent molecules that were identified in the active site of the native enzyme are missing in the P54 mutant structure: (1) the water molecule located in the oxyanion hole (Wat22 in 3BLM) and (2) the water molecule to which we have assigned a role in the deacylation of the substrate (Wat81 in 3BLM; Herzberg & Moult, 1987; Herzberg, 1991). It is not clear why the first water molecule is missing; however, the second one interacts with the side chains of Glu166 and Asn170 in the native structure, and their apparent disorder in P54 eliminates its electrostatically favorable niche.

(C) *Effects on Kinetics.* Stopped-flow observations of the hydrolysis on nitrocefin in the presence of P54 showed a fast first phase that rapidly declined, presumably to the steady-state rate. A large excess of enzyme over substrate is necessary to reduce the kinetics to those of a simple first-order process (Laidler & Bunting, 1973). For P54, the first-order rate constants under these conditions changed slowly with enzyme concentration in the range 50–90 μM (substrate concentration 20 μM), and extrapolation to infinite enzyme concentration allows k_{+2} to be estimated as 21.5 s^{-1}. Under similar conditions the first-order rate constant for PC1 was estimated as 200 s^{-1}.

Thus the fast phase, corresponding roughly to k_{+2}, occurs only 10 times faster for PC1 than for P54. In contrast, the steady-state turnover rate with P54 was sharply reduced. k_{cat} fell from 11.4 s^{-1} with PC1 to 0.02 s^{-1} for P54. With the stopped-flow observations, this implies that for P54 $k_{+3} \ll k_{+2}$ and $k_{+3} \simeq k_{cat}$. The K_m's were 6.9×10^{-6} M (PC1) and 2.0×10^{-6} M (P54).

The effect of changing pH and ammonium sulfate concentration on the rate of hydrolysis of penicillin G by PC1 and P54 is summarized in Table V. The rate is reduced for PC1 when the pH is increased to 8.0; however, it remains constant between pH 5 and 6.8. In addition, although K_m was too low to be measured accurately, there was an indication of reduced values at pH 5.5 and 5.0, which we attribute to a slow inactivation of the enzyme. In contrast to native PC1, the relative rate of hydrolysis by P54 is increased 4.5-fold when the pH is lowered from 6.8 to 5.0, whereas when the pH is increased to 8.0 the rate is reduced by a factor similar to that for PC1. K_m did not appear to be affected by pH in P54. Both enzymes show an increase in rate of catalysis at higher ammonium sulfate concentration, but the effect on P54 is larger.

Table V: Effect of pH and Ammonium Sulfate Concentration on k_{cat} of Penicillin G[a]

	pH				
	5.0	5.5	6.0	6.8	8.0
PC1	333	333	333	333	120
P54	2.9	2.3	1.2	0.6	0.2

	saturated $(NH_4)_2SO_4$		
	0%	30%	60%
PC1	333	390	511
P54	0.6	1.4	4.1

[a] k_{cat} values are given in s^{-1}.

Discussion

The proposal that the Ω-loop regin of β-lactamase is marginally stable is supported by the structure of the P54 mutant. In the native structure the side chain of Asp179 provides enough electrostatic interactions to balance the destabilizing effects of the relatively inefficient packing of the loop against the rest of the molecule and of the steric strain caused by the cis peptide between Glu166 and Ile167 (Herzberg, 1991; Herzberg & Moult, 1991). The carboxylate moiety of Asp179 is inaccessible to solvent and is involved in two types of interactions that also bury the charge: (1) a salt bridge with the side chain of Arg164 and (2) electrostatic interactions with the main-chain nitrogen atoms of Val163 and Arg164, whose dipoles are oriented toward each other. These interactions are not possible once the aspartate is replaced by an asparagine residue, and an alternate conformtion of the asparagine side chain is preferred, resulting in the disordering of the loop and the inactivation of the enzyme.

Craig et al. (1985) have shown by differential sedimentation experiments that P54 is less compact then the native PC1 β-lactamase; the Stokes radius of the P54 mutant is about 7% larger than that of PC1. We propose that the lack of a uniquely folded compact conformation of the Ω-loop accounts for this expansion. The folding kinetics in guanidinium chloride of the native and the P54 mutant β-lactamases have also been studied by Craig et al. (1985), leading to the proposal that states H and I of the wild-type enzyme are on the folding pathway of the enzyme and that the mutant structure has been blocked in a conformation that, in the properties so far determined, resembles state I. If such is the case, and with the knowledge of the X-ray structures of both the native and the P54 mutant proteins, it is expected that the cis–trans isomerization of the peptide bond between Glu166 and Ile167 should be the rate-limiting step in the conversion from the conformational state I to the native state. Further kinetic studies of the folding of PC1, looking for this cis–trans isomerization, could confirm this or otherwise would show that intermediate I represents a folding state distinct in conformation from P54.

The partial recovery of the activity of P54 at lower pH or higher ammonium sulfate concentration may be interpreted in two ways: (1) deacylation is restored by a mechanism that does not involve Glu166 and is assisted by protons or salt ions or (2) salt and low pH provide additional stability to the Ω-loop of P54, recovering some of its deacylation function. Sulfate ions have been shown to reverse the unfolding of native PC1 β-lactamase by urea and to stabilize the folded state (Mitchinson & Pain, 1985). The increased solvent screening

due to high salt concentration may reduce the effect of the unfavorable electrostatic interaction between the main-chain nitrogen atoms of Val163 and Arg164, caused by the mutation, such that the Ω-loop could sample its native conformation more frequently. The recovered activity is rather low, though, consistent with the Ω-loop appearing disordered in the crystal in spite of its high ammonium sulfate concentration. In contrast, it is difficult to envisage how low pH could have a stabilizing effect on the loop in this manner.

A proposal pertaining to the residual activity of the mutant enzyme has been derived on the basis of the analysis of the P54 crystal structure: If as suggested previously (Herzberg & Moult, 1987) Glu166 is involved in deacylation, and since this amino acid residue is disordered in the P54 structure, one would expect that the rate-limiting step in the hydrolysis of β-lactams by P54 should be the deacylation of the substrate. In contrast, Martin and Waley (1988) found a similar pH dependence of k_{+2} and k_{+3} of the closely related *Bacillus cereus* β-lactamase and argues that this indicates that the same enzyme groups participate in catalysis of both acylation and deacylation. They suggested that Glu166 plays this double role. Such a mechanism implies that both steps would also be affected in P54.

The stopped-flow observations give direct support to our model, since the reduction in the rate of the first phase is much less than the effect on k_{cat}. Thus, we have shown that the two halves of the reaction are functionally separate, with the acylation step distinct from the deacylation step. This is consistent with our proposal that Glu166 is involved only in the deacylation of the enzyme by enhancing the nucleophilicity of a solvent molecule that is adjacent to it and to the acylated seryl residue.

This work also pertains to the differences between the serine protease family (Kraut, 1977) and the β-lactamases. Although in both cases catalysis progresses via a seryl acyl enzyme and there is an oxyanion hole involved in stabilizing the negatively charge tetrahedral conformer, the assisting apparatus is different: (1) Instead of the catalytic histidyl residue of the serine proteases, in class A β-lactamases Lys73 and Ser130 are located in a similar position (Herzberg & Moult, 1987; Herzberg, 1990). (2) β-Lactamase lacks the buried aspartyl residue that interacts with the catalytic histidine in the serine proteases. (3) Glu166 is unique to the class A β-lactamases. Thus, unlike the serine proteases, where the deacylation is believed to be achieved by simple reversal of the acylation step (with a water molecule replacing the leaving amine), here the two steps are assisted by different groups.

The structural basis for the activation of trypsin (Huber & Bode, 1978) is reminiscent of the β-lactamase P54/PC1 case. The zymogen—trypsinogen—is inactive, and activation occurs when the N-terminal peptide is cleaved. Whereas in trypsinogen there are four loop segments close to the active site that are invisible in the electron density map, in the crystal structure of trypsin these are well ordered. The activation is achieved by the salt bridge between the new α-amino group of the cleaved protein and a buried aspartyl residue. Since this α-amino group does not exist in the zymogen, the aspartate adopts a different conformation that facilitates alternative electrostatic interaction. Other conformational transitions are involved, ultimately leading to the disordering of the four loops. Such conformational transition due to stabilization by a salt bridge is analogous to the transition of the Ω-loop from the inactive form of P54 to the active form of native PC1. Unlike trypsinogen, where the oxyanion binding site appears to be substantially distorted, in P54 the shifts of the oxyanion hole atoms are somewhat coupled and more subtle to interpret.

ACKNOWLEDGMENTS

We thank John Moult for many helpful discussions, Richard P. Ambler and Margaret Daniel for repeating the sequence analysis of P54 and for confirming its correctness, and S. G. Chapman for the use of his stopped-flow apparatus.

REFERENCES

Ambler, R. P. (1975) *Biochem. J. 151*, 197–218.
Ambler, R. P. (1979) in *Beta-Lactamases* (Hamilton-Miller, J. M. T., & Smith, J. T., Eds.) pp 99–125, Academic Press, London.
Ambler, R. P., Coulson, A. F. W., Forsman, M., Tiraby, G., Frêre, J.-M., Ghuysen, J. M., Joris, B., Levesque, R. C., & Waley, S. G. (1991) *Biochem. J. 276*, 269–272.
Bernstein, F. C., Koetzle, T. F., Williams, G. J. B., Meyer, E. F., Jr., Brice, M. D., Rodgers, J. R., Kennard, O., Shimanouchi, T., & Tasumi, M. (1977) *J. Mol. Biol. 112*, 535–542.
Bhat, T. N. (1988) *J. Appl. Crystallogr. 21*, 279–281.
Carrey, E. A., & Pain, R. H. (1978) *Biochim. Biophys. Acta 533*, 12–22.
Christensen, H., Martin, M. T., & Waley, S. G. (1990) *Biochem. J. 266*, 853–861.
Coulson, A. (1985) *Biotechnol. Genet. Eng. Rev. 3*, 219–253.
Craig, S., Hollecker, M., Creighton, T. E., & Pain, R. H. (1985) *J. Mol. Biol. 185*, 681–687.
Creighton, T. E., & Pain, R. H. (1980) *J. Mol. Biol. 137*, 431–436.
Finzel, B. C. (1987) *J. Appl. Crystallogr. 20*, 53–55.
Hendrickson, W. A., & Konnert, J. H. (1980) in *Biomolecular Structure, Function, Conformation and Evolution* (Srinivasan, R., Ed.) Vol. 1, pp 43–75, Pergamon Press, Oxford, England.
Herzberg, O. (1991) *J. Mol. Biol. 217*, 701–719.
Herzberg, O., & Moult, J. (1987) *Science 236*, 694–701.
Herzberg, O., & Moult, J. (1991) *Proteins: Struct., Funct., Genet.* (in press).
Howard, A. J., Gilliland, G. L., Finzel, B. C., Poulos, T., Ohlendorf, D. O., & Salemme, F. R. (1987) *J. Appl. Crystallogr. 20*, 383–387.
Huber, R., & Bode, W. (1978) *Acc. Chem. Res. 11*, 114–122.
Jones, T. A. (1982) in *Computational Crystallography* (Sayre, D., Ed.) pp 303–317, Oxford University Press, London and New York.
Kraut, J. (1977) *Annu. Rev. Biochem. 46*, 331–358.
Laidler, K. J., & Bunting, P. S. (1973) *Chemical Kinetics of Enzyme Action*, Clarendon Press, Oxford, England.
Martin, M. T., & Waley, S. G. (1988) *Biochem. J. 254*, 923–925.
Mitchinson, C., & Pain, R. H. (1985) *J. Mol. Biol. 184*, 331–342.
Moult, J., Sawyer, L., Herzberg, O., Jones, C. L., Coulson, A. E. W., Green, D. W., Harding, M. M., & Ambler, R. P. (1985) *Biochem. J. 225*, 167–176.
Novick, R. P. (1963) *J. Gen. Microbiol. 33*, 121–136.
Robson, B., & Pain, R. H. (1976a). *Biochem. J. 155*, 325–330.
Robson, B., & Pain, R. H. (1976b). *Biochem. J. 155*, 331–344.